# A Novel Simplified Four-Port Scattering Parameter Model for Design of Four-Pair Twisted-Pair Cabling Systems for Local Area Networks

Chun-Wen Paul Huang, Charles E. Smith, *Life Senior Member, IEEE*, Atef Z. Elsherbeni, *Senior Member, IEEE*, and Bernard H. Hammond, Jr.

***Abstract*—This paper presents a set of simplified equations based on a four-port scattering model, which accurately characterizes four-pair twisted pair (eight-port) cabling systems for high-speed digital telecommunication local area networks. These equations are derived and simplified from two-stage cascaded four-port $S$-parameter matrices and verified experimentally. Excellent agreement is obtained between the measurements and computational results when the $S$-parameters of the cabling system components are known. These equations not only reduce the computation burdens in comparison with traditional methods for transmission matrix computations, but also provide intuition of the contributions of the $S$-parameters at each stage in the net crosstalk, return loss, and insertion loss. Furthermore, these equations can be used to compute the component specifications when the system performance is specified, and to obtain the deembedded system characteristics by subtracting the known characteristics of adapters.**

***Index Terms*—Four-port scattering parameters, twisted-pair cabling system.**

## I. Introduction

With the recent advancements of digital technologies, tremendous demands have been made to improve the computer networking systems. Inside buildings, most current local area networks (LAN's) are built by interconnecting workstations, personal computers, and telecommunication hubs with cabling systems. These cabling systems are lossy multiconductor transmission lines, in which high-speed digital signals are always severely distorted after traveling through the cabling systems. This distortion is due to the relative small signal-to-noise ratio at the higher frequency spectra, which results from both the enormous propagation attenuation and pair-to-pair crosstalk. The small signal-to-noise ratio at high-frequency spectra of imperfect cabling systems limits the networking speed and increases the design profile of networking interface circuitry, especially for echo and crosstalk canceling and signal error corrections. The most widely adopted cabling systems in LAN's today are the four-pair (eight conductors) twisted pair cables and connecting hardware, which are always characterized using scattering parameters ($S$-parameters), mainly in differential mode [1]. The cabling system qualifications are also done by measuring the $S$-parameters of the systems. Numerous field and laboratory tests are done for installation qualification and system designs. Therefore, there is a need to develop a simulation model to not only predict cabling system performance when the components are specified, but also to provide insights for the interactions between the $S$-parameters of each component in the system.

In most circuit simulators, the transmission matrix method [2] is adopted to calculate the system performance of a cascaded multistage circuit when the component at each stage is specified. For simulating a multiport cascaded system, the transmission matrix at each stage, defined in voltage and current at each port, is multiplied with the next stage, and the product matrix of all transmission matrices represents the characteristics of the cascaded multiport system. However, cabling components and systems are characterized in scattering parameter [1] instead of voltages and currents. In [3], methods are introduced to re-express the transmission matrices in scattering parameters and the transformation of transmission parameters to $S$-parameters. Therefore, the $S$-parameter measurements of cabling components can be used for simulation. Using the transmission matrix method with transmission parameters for $S$-parameter transformation to characterize a multistage cabling system, an $8 \times 8$ matrix operation is required. However, there are two major disadvantages when using the $8 \times 8$ transmission matrices to model the cabling system. When evaluating the system's crosstalks, systems are often tested partially on the worst crosstalk pairs, which are between the pair connected to contacts number 3 and 6 and the pair connected to contacts number 4 and 5 of an RJ-45 connecting hardware. Therefore, the eight-port transmission matrix model is too cumbersome to predict the system performance, especially when only the systems are partially tested. In addition, the computed cascaded results cannot provide the insights between the parameters of components at each junction, which is very important information for component and system designs to fine tune the component characteristics to meet the system specifications.

In this paper, a four-port scattering parameter model is presented and verified to accurately predict all the test parameters of two crosstalk pairs in a four-pair (eight-port) multistage cascaded cabling system. The proposed equations of this four-port model are simplified from a two-stage cascaded four-port scattering matrix. With this model, four-pair (eight-port) cabling

Manuscript received March 5, 1999.

C.-W. P. Huang, C. E. Smith, and A. Z. Elsherbeni are with the Electrical Engineering Department, University of Mississippi, University, MS 38677 USA (e-mail: atef@olemiss.edu).

B. H. Hammond, Jr. is with the Thomas and Betts Corporation, Memphis, TN 38125 USA.

Publisher Item Identifier S 0018-9480(00)03764-9.

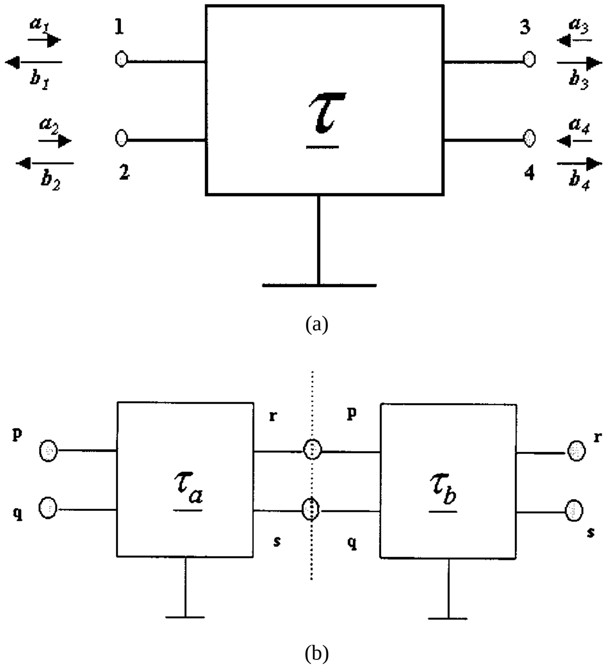


Fig. 1. Four-port scattering parameter model for: (a) unintary stage transmission matrix and (b) two-stage cascaded transmission matrices.

systems are not only accurately modeled by a much simplified four-port model, but also provide the insights of the interactions between $S$-parameters from each component. These equations can be applied to obtained deembedded system performance with the characteristics of known adapters and to compute component characteristics to meet system specifications.

## II. Methodology

The proposed four-port method is a simplified model based on the characteristics of current cabling components. From the current standards for cabling components outlined in [4], the product of two or more crosstalks and the five or more return losses (RL's) are negligible within the whole frequency spectra. When measuring the pair-to-pair crosstalk in a four-pair twisted-pair system, the coupling coefficient is measured by the ratio of the induced voltage on a quiet pair and the exciting voltage on the excited pair. The induced voltages on the other two quiet pairs of the four-pair twisted-pair system have insignificant contribution on the pair-to-pair coupling of the two pairs under study, because the product of two crosstalks is negligible. Therefore, when modeling pair-to-pair crosstalks in a four-pair twisted-pair system, a four-port (two-pair) model can be used instead of using an eight-port model. However, the characteristics of the original eight-port system still exist in the characteristic impedance of each port and the pair-to-pair coupling capacitance and inductance.

Using the above outlined simplification criteria, a four-port transmission matrix model for modeling the crosstalk between any two adjacent pairs of a four-pair twisted pair system is shown in Fig. 1(a). The transmission matrix used in the proposed four-port model is expressed in $S$-parameters instead of voltage and current. Therefore, to utilize the four-port transmission matrix method when the measurements are in $S$-parameters, the four-port transformations of $S$-parameter matrix to the transmission matrix and the transmission matrix to $S$-parameter matrix are necessary. The methodology can be found in [3]. The transmission matrix in terms of $S$-parameters is obtained from the following two equations:

$$|b\rangle = \underline{S} \cdot |a\rangle \tag{1}$$

where $\underline{S}$ is the $S$-parameter matrix of a four-port system, $|a\rangle$ is the vector of the incident wave amplitude, and $|b\rangle$ is the vector of the reflected wave amplitude. The $S$-parameter formated transmission matrix may be defined as [3]

$$\begin{pmatrix} b_1 \\ b_2 \\ a_1 \\ a_2 \end{pmatrix} = \underline{\tau} \cdot \begin{pmatrix} a_3 \\ a_4 \\ b_3 \\ b_4 \end{pmatrix} \tag{2}$$

where the components $a_i$ and $b_i$ are the incident and reflected wave amplitudes at port $i$, respectively. The matrix $\underline{\tau}$ is the transmission matrix defined for $S$-parameters. Utilizing Mathematica Version 5 to reexpress (1) into the format of (2), the $S$-parameter formated transmission matrix $\underline{\tau}$ can be obtained. The first row of $\underline{\tau}$ is then given by

$$\tau_{11} = S_{13} - \frac{S_{12}S_{33}S_{41}}{S_{32}S_{41} - S_{31}S_{42}} + \frac{S_{11}S_{33}S_{42}}{S_{32}S_{41} - S_{31}S_{42}} + \frac{S_{12}S_{31}S_{43}}{S_{32}S_{41} - S_{31}S_{42}} - \frac{S_{11}S_{32}S_{43}}{S_{32}S_{41} - S_{31}S_{42}} \tag{3a}$$

$$\tau_{12} = S_{14} - \frac{S_{12}S_{34}S_{41}}{S_{32}S_{41} - S_{31}S_{42}} + \frac{S_{11}S_{34}S_{42}}{S_{32}S_{41} - S_{31}S_{42}} + \frac{S_{12}S_{31}S_{44}}{S_{32}S_{41} - S_{31}S_{42}} - \frac{S_{11}S_{32}S_{44}}{S_{32}S_{41} - S_{31}S_{42}} \tag{3b}$$

$$\tau_{13} = \frac{S_{12}S_{41}}{S_{32}S_{41} - S_{31}S_{42}} - \frac{S_{11}S_{42}}{S_{32}S_{41} - S_{31}S_{42}} \tag{3c}$$

$$\tau_{14} = -\frac{S_{12}S_{31}}{S_{32}S_{41} - S_{31}S_{42}} + \frac{S_{11}S_{32}}{S_{32}S_{41} - S_{31}S_{42}} \tag{3d}$$

where $S_{11}, \cdots, S_{44}$ are associated with the reflection coefficients, $S_{31}$ and $S_{42}$ are associated with the transmission coefficients of the four-port model, $S_{12}$ and $S_{43}$ represent the near-end coupling coefficients, and $S_{32}$ and $S_{41}$ are far-end coupling coefficients. However, (3) can be simplified by neglecting all the product of any two or more crosstalk coefficients. Thus,

$$\tau_{11} = S_{13} - \frac{S_{11}S_{33}S_{42}}{S_{31}S_{42}} \tag{4a}$$

$$\tau_{12} = S_{14} - \frac{S_{11}S_{34}S_{42}}{S_{31}S_{42}} - \frac{S_{12}S_{31}S_{44}}{S_{31}S_{42}} + \frac{S_{11}S_{32}S_{44}}{S_{31}S_{42}} \tag{4b}$$

$$\tau_{13} = \frac{S_{11}S_{42}}{S_{31}S_{42}} \tag{4c}$$

$$\tau_{14} = -\frac{S_{12}S_{31}}{S_{31}S_{42}} - \frac{S_{11}S_{32}}{S_{31}S_{42}}. \tag{4d}$$

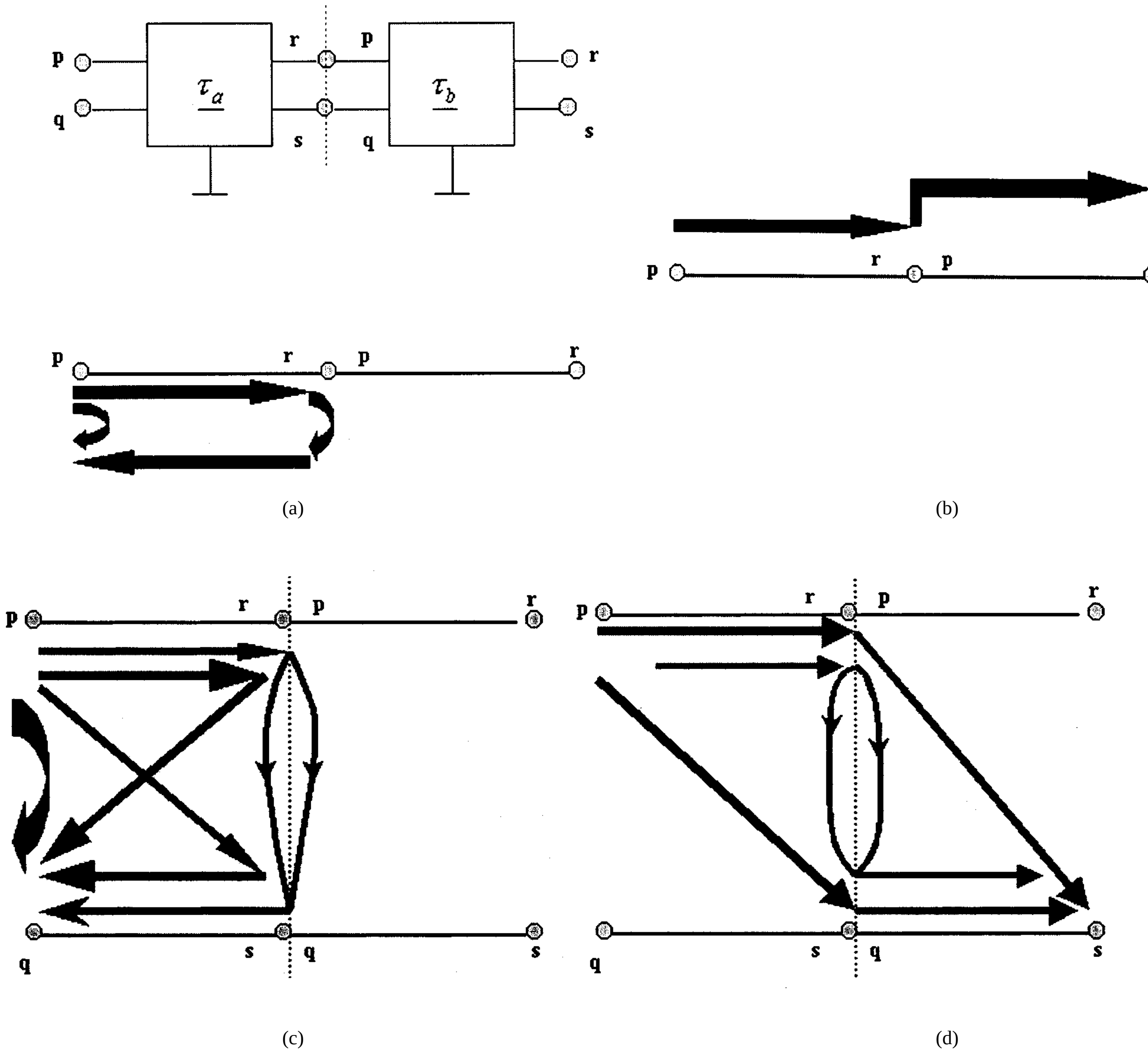


Fig. 2. Signal-flow interpretations for: (a) $Sn_{pp}$, (b) $Sn_{rp}$, (c) $Sn_{qp}$, and (d) $Sn_{sp}$.

For a multistage four-port cascade system, the final transmission matrix can be obtained by using

$$\underline{\tau_n} = \underline{\tau_a} \cdot \underline{\tau_b} \cdot \underline{\tau_c}, \cdots. \tag{5}$$

After cascading all the transmission matrices in a system, the final transmission matrix is needed to be transformed into the scattering matrix, which can be done by re-expressing (2) into the format of (1). The first row of the $S$-matrix in terms of transmission parameters are shown in (6a)–(6d), at the bottom of the following page.

To derive explicit expressions for the components of a multistage cascaded $S$-matrix, the transmission matrices of arbitrary two stages $\underline{\tau_a}$ and $\underline{\tau_b}$ are cascaded and transformed to the scattering matrix. The two-stage cascaded $S$-matrix is simplified by using the simplification criteria outlined above. All the simplifications and reorganizing of terms in matrices are done using Mathematica Version 5. The four-port cascade model for any two stages is shown in Fig. 1(b), when ports $p$, $r$, $q$, and $s$ represent two arbitrary crosstalk pairs in a four-pair cabling system. The simplified $S$-parameters of the two-stage cascaded four-port model are introduced as follows, where $Sn_{ij}$ denotes the two-stage cascaded results of $S_{ij}$. The $Sn_{pp}$ term, associated with the reflection coefficient at port $p$, is

$$Sn_{pp} = Sa_{pp} + \frac{Sa_{rp}Sb_{pp}Sa_{pr}}{1 - Sa_{rr}Sb_{pp}} \tag{7}$$

where $n$ represents the cascade results.

The $Sn_{rp}$ term, associated with the transmission coefficient between ports $p$ and $r$, is

$$Sn_{rp} = \frac{Sa_{rp}Sb_{rp}}{1 - Sa_{rr}Sb_{pp}}. \tag{8}$$

The $Sn_{qp}$, associated with the near-end coupling coefficient between port $p$ and $q$, is expressed as

$$Sn_{qp} = Sa_{qp} + \frac{Sa_{rp}Sb_{pp}Sa_{qr}}{1 - Sa_{rr}Sb_{pp}} + \frac{Sa_{sp}Sb_{qq}Sa_{sq}}{1 - Sa_{ss}Sb_{qq}} + \frac{Sa_{rp}(Sb_{qp} + Sb_{pp}Sa_{sr}Sb_{qq})Sa_{qs}}{(1 - Sa_{rr}Sb_{pp})(1 - Sa_{ss}Sb_{qq})}. \tag{9}$$

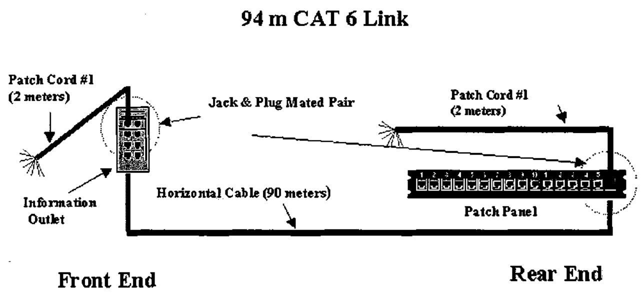


Fig. 3. Device-under-test: a 94-m CAT 6 (up to 250 MHz) telecommunications permanent link.

The $Sn_{sp}$, associated with the far-end coupling coefficient between port $p$ and $s$, is

$$Sn_{sp} = \frac{Sa_{rp}Sb_{sp}}{1 - Sa_{rr}Sb_{pp}} + \frac{Sa_{sp}Sb_{sq}}{1 - Sa_{ss}Sb_{qq}} + \frac{Sa_{rp}(Sb_{pp}Sa_{sr} + Sb_{qp}Sa_{ss})Sb_{sq}}{(1 - Sa_{rr}Sb_{pp})(1 - Sa_{ss}Sb_{qq})} \quad (10)$$

where $a$ and $b$ in the $S$-parameters represent the first and second stages, respectively, in a cascaded system. However, in computation, the previous two cascaded results can be treated as a new stage $a$ and the next stage can be treated as $b$. If only the characteristics of the system worst crosstalk pairs in the cabling system are studied, then the cascaded characteristics can be obtained by applying (7)–(10) thorough all the stages directly. The full characteristics of a multistage eight-port cascaded system can be obtained by applying (9) and (10) to all the pair-to-pair combinations and by applying (7) and (8) to all of the four pairs. Identical equations can also be obtained by using the signal-flow graph method with Mason's nontouching loop rules [5]. The signal-flow interpretations of (7)–(10) are shown in Fig. 2.

From the signal-flow interpretation of (7)–(10) in Fig. 2, some important concepts can be observed that also agree with measurement experiences for cabling systems. The RL at each port (pair) is determined primarily by the characteristic impedance at each stage and junction mismatch, as shown in Fig. 2(a). The crosstalks do not significantly impact the RL measurements. The insertion loss (IL) is only determined by the IL at each stage and the junction mismatch, as shown in Fig. 2(b), and the crosstalks do not have an impact on the IL. As shown in Fig. 2(c), the near-end cross talk (NEXT) is determined by the NEXT at the first stage, and the NEXT at later stages are directly added to the front stage after being attenuated by the IL at the former stage, when the junction mismatch is small. From (9), the relation between NEXT and far-end cross talk (FEXT) are also observed. The signal reflected from the junction mismatch will be added to the NEXT through FEXT of the former stage. As shown in Fig. 2(d), the FEXT is determined by the possible signal transmission paths of the far end to the near end. NEXT's are also added to the cascaded FEXT when the junction is mismatched. Therefore, the relations of the $S$-parameters at each stage are shown in (7)–(10), which may provide insights for both system and component designs.

All the parameter used in (7)–(10) are in complex formats. However, most component characteristics provided by manufacturers are magnitude measurements only, which are insufficient for (7)–(10). However, (7)–(10) can be rewritten in terms of magnitudes in phase to predict the system worst-case performance. The equations for worst-case predictions are expressed as

$$|Sn_{pp}| = |Sa_{pp}| + \frac{|Sa_{rp}||Sb_{pp}||Sa_{pr}|}{1 - |Sa_{rr}||Sb_{pp}|} \quad (11)$$

$$|Sn_{rp}| = \frac{|Sa_{rp}|\,|Sb_{rp}|}{1 + |Sa_{rr}|\,|Sb_{pp}|} \quad (12)$$

$$|Sn_{qp}| = |Sa_{qp}| + \frac{|Sa_{rp}|\,|Sb_{pp}|\,|Sa_{qr}|}{1 - |Sa_{rr}|\,|Sb_{pp}|} + \frac{|Sa_{sp}|\,|Sb_{qq}|\,|Sa_{sq}|}{1 - |Sa_{ss}|\,|Sb_{qq}|} + \frac{|Sa_{rp}|\,(|Sb_{qp}| + |Sb_{pp}|\,|Sa_{sr}|\,|Sb_{qq}|)\,|Sa_{qs}|}{(1 - |Sa_{rr}|\,|Sb_{pp}|)(1 - |Sa_{ss}|\,|Sb_{qq}|)} \quad (13)$$

$$|Sn_{sp}| = \frac{|Sa_{rp}|\,|Sb_{sp}|}{1 - |Sa_{rr}|\,|Sb_{pp}|} + \frac{|Sa_{sp}|\,|Sb_{sq}|}{1 - |Sa_{ss}|\,|Sb_{qq}|} + \frac{|Sa_{rp}|(|Sb_{pp}|\,|Sa_{sr}| + |Sb_{qp}|\,|Sa_{ss}|)|Sb_{sq}|}{(1 - |Sa_{rr}|\,|Sb_{pp}|)(1 - |Sa_{ss}|\,|Sb_{qq}|)}. \quad (14)$$

---

$$S_{11} = \frac{\tau_{14}\tau_{43} - \tau_{13}\tau_{44}}{\tau_{34}\tau_{43} - \tau_{33}\tau_{44}} \quad (6a)$$

$$S_{12} = \frac{-\tau_{14}\tau_{33} + \tau_{13}\tau_{34}}{\tau_{34}\tau_{43} - \tau_{33}\tau_{44}} \quad (6b)$$

$$S_{13} = \frac{\tau_{14}\tau_{33}\tau_{41} - \tau_{13}\tau_{34}\tau_{41} - \tau_{14}\tau_{31}\tau_{43} + \tau_{11}\tau_{34}\tau_{43} + \tau_{13}\tau_{31}\tau_{44} - \tau_{11}\tau_{33}\tau_{44}}{\tau_{34}\tau_{43} - \tau_{33}\tau_{44}} \quad (6c)$$

$$S_{14} = \frac{\tau_{14}\tau_{33}\tau_{42} - \tau_{13}\tau_{34}\tau_{42} - \tau_{14}\tau_{32}\tau_{43} + \tau_{12}\tau_{34}\tau_{43} + \tau_{13}\tau_{32}\tau_{44} - \tau_{12}\tau_{33}\tau_{44}}{\tau_{34}\tau_{43} - \tau_{33}\tau_{44}} \quad (6d)$$

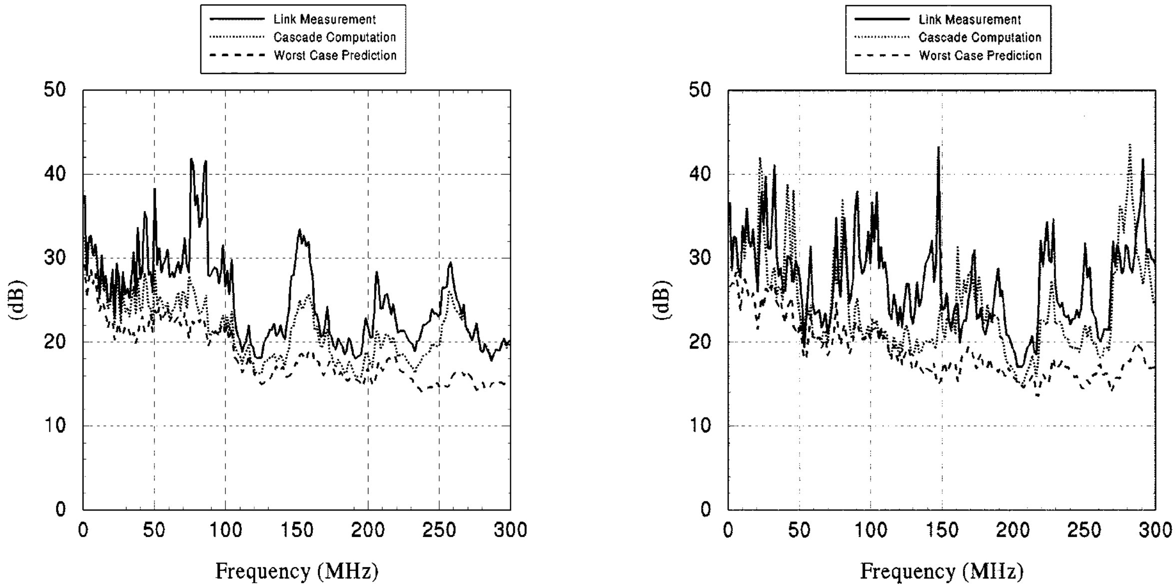


(a) (b)

Fig. 4. RL of the link measurements and cascade computations at the front end. (a) Contacts 3 and 6. (b) Contacts 4 and 5.

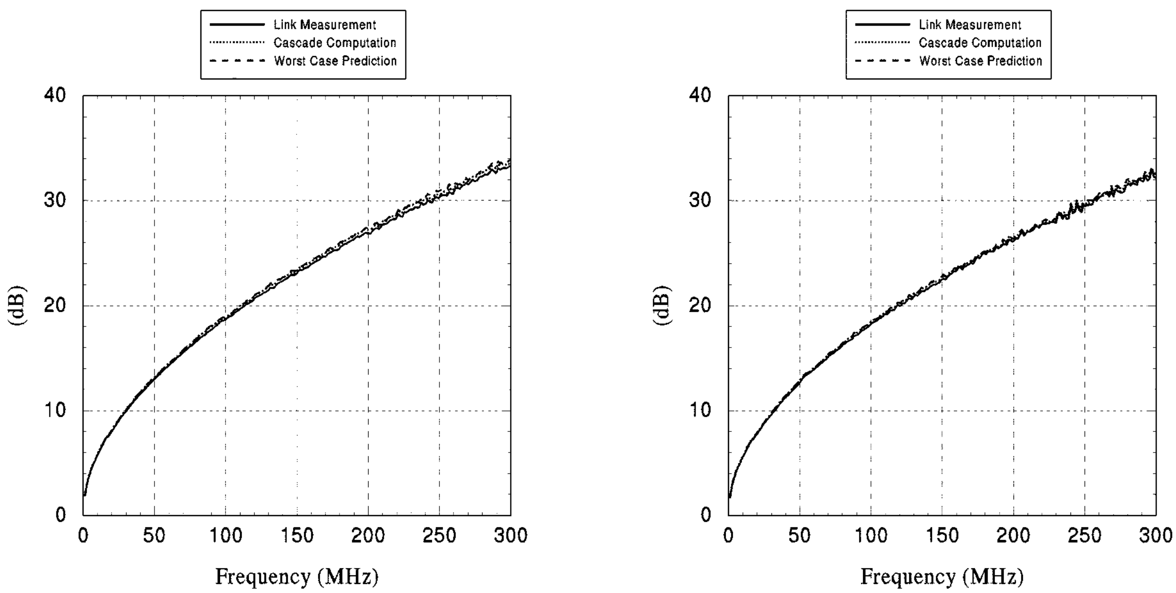


(a) (b)

Fig. 5. IL of the link measurements and cascade computations measured from the front end. (a) Contacts 3 and 6 to the rear-end contacts 3 and 6. (b) Contacts 4 and 5 to the rear-end contacts 4 and 5.

Therefore, even when component characteristics are limited in magnitude measurements, the system can be estimated for its worst case utilizing (11)–(14).

## III. Validations

A category 6 (CAT 6), used up to 200 or 250 MHz, telecommunication permanent link is built to verify the effectiveness of these equations up to 300 MHz. The link consists of two 2-m patch cables at each end, two RJ-45 connectors, and 90-m horizontal cable, as shown in Fig. 3. The test equipment is an HP 8753 D network analyzer with two baluns at each port. For link testing, the patch cable ends are modified to four test lead pairs to connect with baluns in the network analyzer setup. The link is partially tested at the worst crosstalk pairs, which are the pair of connector contact 3 and 6 and the pair of connector contacts 4 and 5. After the link testing is done, the system is divided into five individual stages, which are two patch cables, two connectors, and the horizontal cable. The individual components are measured under the same procedures. The cascade and worst-case predictions of the link performance is computed using the measurement results at each stage in (7)–(10) and in (11)–(14). Due to the symmetrical structure of the telecommunication link, only the system measurements

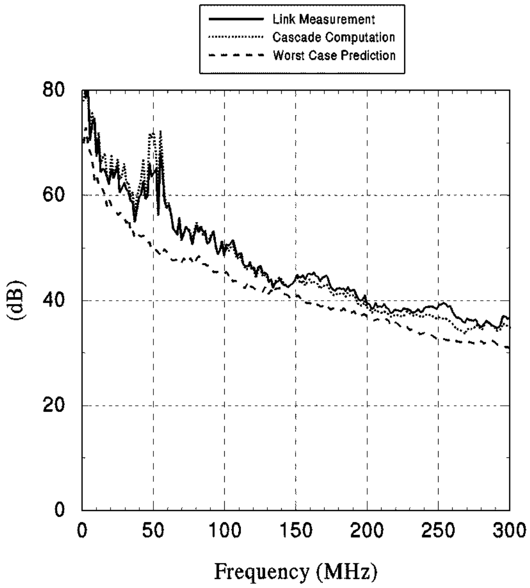


Fig. 6. Near-end crosstalk loss of link measurements and cascade computations measured between the front-end contacts 3 and 6 and contacts 4 and 5.

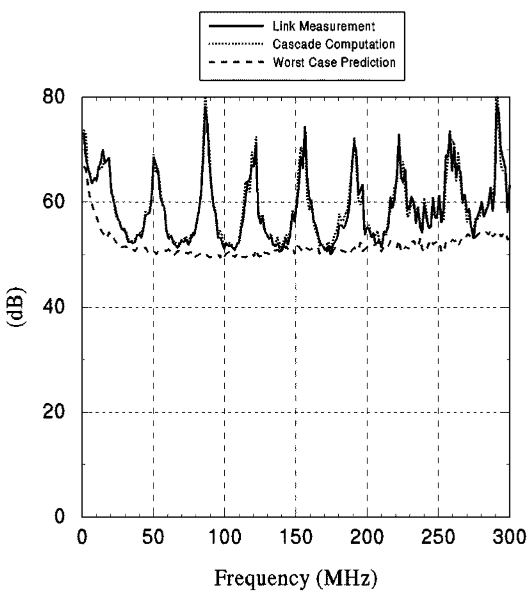


Fig. 7. Far-end crosstalk loss of the link measurements and the cascade computations measured from the front-end contacts 3 and 6 to the rear-end contacts 4 and 5.

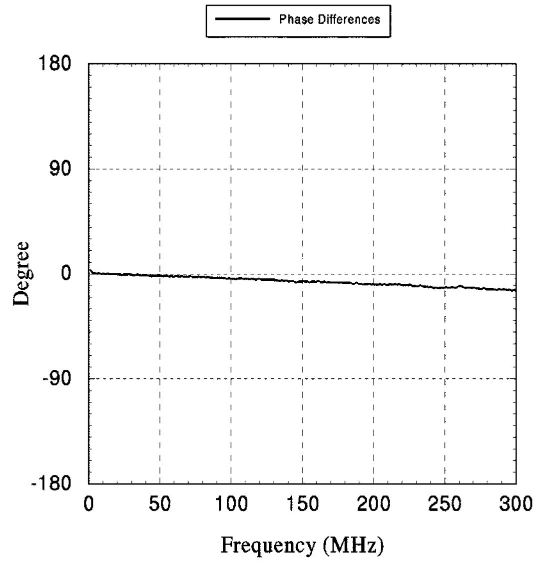


(a)

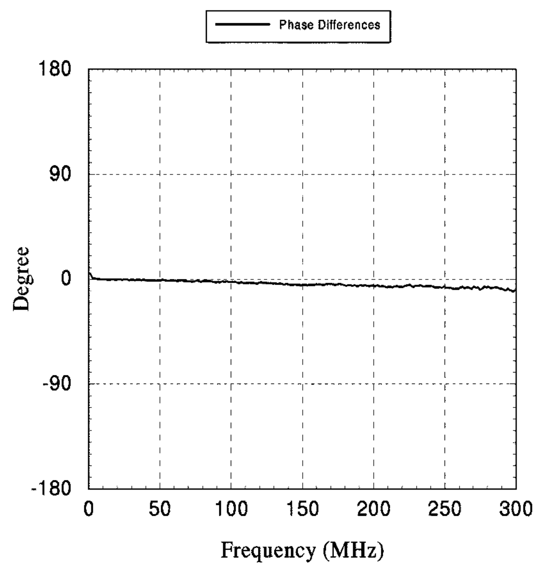


(b)

Fig. 8. Transmission phase differences between the link measurements and cascade computations measured: (a) from the front-end contacts 3 and 6 to the rear-end contacts 3 and 6 and (b) from the front-end contacts 4 and 5 to the rear end contacts 4 and 5.

and computational results at the front end, the information outlet, are shown in Figs. 4–8. The effectiveness of (7)–(10) is proven. The slight differences in RL between measurement and cascaded results are expected, which are due to the changes in the effective cable length of each cable after dividing the link. When measuring each stage, portions of the cables are modified into test lead pairs for the connection between the device-under-test and baluns. In this verification measurement, 12 in of cables are modified into test leads. This change is mainly shown in the input impedance of each cable. However, for IL's, NEXT losses, and FEXT losses, the influences due to the changes of the effective cable lengths are not significant. The equations can accurately model the magnitude and phase of the cascaded system. When evaluating digital systems, delay and delay skew are also important considerations. Equations (11)–(14) also show the effectiveness for the system worst-case predictions. For IL measurements, the computational results from (8) and (12) have very slight differences. Therefore, for IL predictions, (12) with magnitude measurements is very effective and efficient. For other test parameters, the differences between complex models and worst-case predictions are detectable. At some frequency points, the computational results from the complex cascade model and the worst-case predictions are overlapped on each other, which means all the vectors are almost in phase at that frequency. However, both the system measurements and cascaded computations are worse than the worst-case prediction results. The delay of the system is determined by the phase change of the system transmission. Fig. 8 shows insignificant difference between the phase of the link measurement and the phase on the cascaded computation. Therefore, (7)–(10) are a very accurate and intuitive model for current cabling systems. Equations (11)–(14) can also provide effective predictions when information of components is limited in magnitude measurements.

## IV. Conclusions

Simplified equations based on a four-port scattering parameter model for simulating cabling systems are presented and verified in this paper. These equations provide accurate cascade results when components are known and insights of the interactions between $S$-parameters at each stage. In additions, when measurements of the system and the adapter are available, the deembedded system characteristics are also obtainable by re-expressing (7)–(10). These derived equations can be applied to multiport systems when the product of two or more crosstalks and the product of five or more RL's are considered negligible.

## Acknowledgment

The authors would like to thank I. P. Rubin de la Borbolla, Thomas and Betts Corporation, Memphis, TN, for helping in the construction of the telecommunications link and R. Sampson, Thomas and Betts Corporation, Memphis, TN, for Fig. 3.

## References

[1] *Commercial Building Telecommunications Cabling Standard*, TIA Standard TIA/EIA-568-A, Oct. 1995.
[2] D. M. Pozar, *Microwave Engineering*. Reading, MA: Addison-Wesley, 1993, pp. 231–234.
[3] D. Kajfez, *Notes on Microwave Circuits*. Oxford, U.K.: Kajfez Consulting, 1989, vol. 1, pp. 243–250.
[4] H. Koeman, "Overview proposed performance specifications for CAT 5, CAT 5E, CAT 6, and CAT 7 cabling NEXT loss, attenuation, ELFEXT loss, and return loss," presented at the ISO/IEC 1998 Meeting.
[5] D. Kajfez, *Notes on Microwave Circuits*. Oxford, U.K.: Kajfez Consulting, 1989, vol. 2, pp. 1–17.

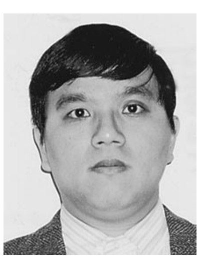

**Chun-Wen Paul Huang** was born in Taipei, Taiwan, R.O.C., on October 18, 1967. He received the diploma in electronic engineering from the National Taipei Institute of Technology, Taipei, Taiwan, R.O.C., in 1991, the M.S. degree in electrical engineering from the University of Mississippi, University, in 1994, and the Ph.D. degree in electrical engineering from the University of Mississippi, in 1999.

From 1991 to 1993, he served as an army officer in charge of wire and wireless telecommunication systems and technologies at the Kaohsiung Regiment Control Area Command, Kaohsiung, Taiwan, R.O.C. He is currently with the Thomas and Betts Corporation, Memphis, TN, where he is involved in the analysis and designs of high-speed digital and passive RF devices and subsystems. His research interests are in the analysis and design of RF microwave circuits and high-speed digital devices, and the applications of finite difference time domain (FDTD) for solving electromagnetic problems.

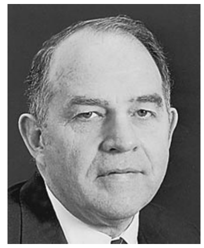

**Charles E. Smith** (M'59–LM'86–LSM'97) was born in Clayton, AL, on June 8, 1934. He received the B.E.E., M.S. and Ph.D. degrees from Auburn University, Auburn, AL, in 1959, 1963, and 1968, respectively.

From 1959 to 1968, he was a Research Assistant with the Auburn University Research Foundation. In late 1968, he became an Assistant Professor of electrical engineering at the University of Mississippi, University, and became an Associate Professor in 1969. He was appointed Chairman of the Department of Electrical Engineering in 1975, and is currently both a Professor and Chair. His main areas of interest are related to the application of electromagnetic theory to microwave circuits and antennas. His recent research has been on the application of numerical techniques to microstrip transmission lines, antenna measurements in lossy media, measurement of electrical properties of materials, computer-aided design (CAD) in microwave circuits, and data acquisition using network analyzers.

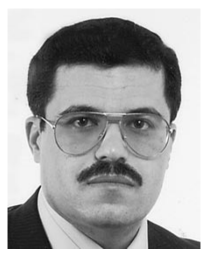

**Atef Z. Elsherbeni** (S'84–M'86–SM'91) received the B.Sc. degree (with honors) in electronics and communications, the B.Sc. degree (with honors) in applied physics, and the M.Eng. degree in electrical engineering from Cairo University, Cairo, Egypt, in 1976, 1979, and 1982, respectively, and the Ph.D. degree in electrical engineering from Manitoba University, Winnipeg, Man., Canada, in 1987.

From 1976 to 1982, he was a Research Assistant with the Faculty of Engineering, Cairo University. From 1983 to 1986, he was a Research Assistant in the Electrical Engineering Department, Manitoba University. From January to August 1987, he was a Post-Doctoral Fellow at Manitoba University. In August 1987, he joined the University of Mississippi, University, as an Assistant Professor of electrical engineering, and in July 1991, he became an Associate Professor and a Professor in July 1997. He spent his first sabbatical term in 1996 with the Electrical Engineering Department, University of California at Los Angeles (UCLA). His professional interests include scattering and diffraction of electromagnetic waves, numerical techniques, antennas, and computer applications for electromagnetic education. He serves on the Editorial Board of the Book Series on "Progress in Electromagnetic Research," the *Electromagnetic Waves and Applications Journal*, the *Computer Applications in Engineering Education Journal*, and *The Applied Computational Electromagnetic Society Journal*.

Dr. Elsherbeni is a member of the Electromagnetics Academy and the Scientific Sigma Xi Society. He serves on the Editorial Board of the IEEE Transactions on Microwave Theory and Techniques.

**Bernard H. Hammond, Jr.** received the B.S.E.E. degree from the Rochester Institute of Technology, Rochester, NY, in 1988.

He is currently the Engineering Manager for the Datacom Division, Thomas and Betts Corporation, Memphis, TN, where he is involved with network and telecommunications interconnect products.